Supplementary Material: Enhancing energy transport utilising permanent molecular dipoles

Adam Burgess[1] and Erik M. Gauger[1]

[1]*SUPA, Institute of Photonics and Quantum Sciences, Heriot-Watt University, Edinburgh, EH14 4AS, UK*

I. Derivation of Hamiltonian

Consider two localised collections of electrical charges A and B, wherein the two charge collections are confined within a distance scale l and are separated by a distance λ. For sufficiently separated collections, $l \ll \lambda$, we can assume that the electromagnetic fields are at the collections' centre of masses $\mathbf{R}_A$ and $\mathbf{R}_B$. In the Coulomb gauge, this leads to a Hamiltonian of the form

$$\begin{aligned} H = &\sum_{\alpha\in A}\frac{1}{2m_\alpha}[\mathbf{p}_\alpha - q_\alpha \mathbf{A}_\perp(\mathbf{R}_A)]^2 \\ &+\sum_{\beta\in B}\frac{1}{2m_\beta}[\mathbf{p}_\beta - q_\beta \mathbf{A}_\perp(\mathbf{R}_B)]^2 \\ &+\sum_{\mathbf{k},n}\omega_{\mathbf{k}} a^\dagger_{\mathbf{k},n}a_{\mathbf{k},n} + V_C^{AA} + V_C^{BB} + V_C^{AB}, \end{aligned} \tag{1}$$

where $\mathbf{p}_i$ is the momentum of the ith charge of strength q_i, $\mathbf{A}_\perp$ is the transverse part of the vector potential. V_C^{ij} is the Coulombic coupling between and amongst the collections A and B. To simplify this Hamiltonian, we utilise the unitary transformation

$$U = \exp\{i\mathbf{d}_A\cdot\mathbf{A}_\perp(\mathbf{R}_A) + i\mathbf{d}_B\cdot\mathbf{A}_\perp(\mathbf{R}_B)\}, \tag{2}$$

$$\mathbf{d}_I = \sum_{i\in I} q_i(\mathbf{r_i} - \mathbf{R}_I), \tag{3}$$

where $\mathbf{d}_{A,B}$ is the dipole operator for the two systems. While this transformation commutes with the position operators and the transverse field operators, it does not commute with the momenta nor field creation and annihilation operators. We have

$$\begin{aligned} U^\dagger \mathbf{p}_\alpha U =&\mathbf{p}_\alpha + q_\alpha \mathbf{A}_\perp(\mathbf{R}_A) \\ &-(\frac{\partial \mathbf{R}_A}{\partial \mathbf{r}_\alpha}\sum_{\alpha'} q_{\alpha'})\cdot\mathbf{A}_\perp(\mathbf{R}_A) + \mathcal{O}(\frac{l}{\lambda}), \end{aligned} \tag{4}$$

for charge neutral collections $\sum_{\alpha'} q_{\alpha'} = 0$, and thus $U^\dagger\mathbf{p}_\alpha U \approx \mathbf{p}_\alpha + q_\alpha\mathbf{A}_\perp(\mathbf{R}_A)$. The unitary acts as a displacement operator on the field annihilation and creation operators

$$U^\dagger a_{\mathbf{k},n} U = a_{\mathbf{k},n} + i\frac{\hat{\mathbf{e}}_n}{\sqrt{2\epsilon_0\omega_{\mathbf{k}}V}}\cdot[\mathbf{d}_A e^{-i\mathbf{k}\cdot\mathbf{R}_A} + \mathbf{d}_B e^{-i\mathbf{k}\cdot\mathbf{R}_B}]. \tag{5}$$

This leads to a total transformed Hamiltonian of the form

$$\begin{aligned} \tilde{H} =&U^\dagger H U \\ =&\sum_{\alpha\in A}\frac{1}{2m_\alpha}\mathbf{p}_\alpha^2 + \sum_{\beta\in B}\frac{1}{2m_\beta}\mathbf{p}_\beta^2 + V_C^{AA} + V_C^{BB} + V_C^{AB} \\ &+\sum_{\mathbf{k},n}\Big(\omega_{\mathbf{k}}[a^\dagger_{\mathbf{k},n}a_{\mathbf{k},n} \\ &+\sum_{S=A,B} i\frac{\hat{\mathbf{e}}_n\cdot\mathbf{d}_S}{\sqrt{2\epsilon_0\omega_{\mathbf{k}}V}}(e^{-i\mathbf{k}\cdot\mathbf{R}_S}a^\dagger_{\mathbf{k},n} - \text{h.c.})] \\ &+\frac{1}{2\epsilon_0 V}\Big[(\hat{\mathbf{e}}_n\cdot\mathbf{d}_A)^2 + (\hat{\mathbf{e}}_n\cdot\mathbf{d}_B)^2 \\ &+(\hat{\mathbf{e}}_n\cdot\mathbf{d}_A)(\hat{\mathbf{e}}_n\cdot\mathbf{d}_B)2e^{i\mathbf{k}\cdot(\mathbf{R}_A-\mathbf{R}_B)}\Big]\Big). \end{aligned} \tag{6}$$

For neutrally charged, well-separated collections of charges, one can show that the cross-coupling terms cancel and assuming that the collections are proximal to each other, such that they fall within a wavelength of light and thus the phase relations are unimportant yields

$$\tilde{H} = H_A + H_B + H_I + H_B, \tag{7}$$

where

$$\begin{aligned} H_{A,B} = &\sum_{\alpha\in A,B}\frac{1}{2m_\alpha}\mathbf{p}_\alpha^2 + V_C^{AA,BB} \\ &+\sum_{\mathbf{k},n}\frac{1}{2\epsilon_0 V}(\hat{\mathbf{e}}_n\cdot\mathbf{d}_{A,B})^2, \end{aligned} \tag{8}$$

$$H_I = -\sum_{S=A,B}\mathbf{d}_S\cdot\mathbf{E}, \tag{9}$$

$$H_B = \sum_{\mathbf{k},n}\omega_{\mathbf{k}}a^\dagger_{\mathbf{k},n}a_{\mathbf{k},n}, \tag{10}$$

and where $\mathbf{E}$ is the electric field operator. Now we truncate the Hilbert space of the collections of charges in A and B to a two-level Hilbert space such that after diagonalising the system Hamiltonians

$$H_{A,B} = \omega_{A,B}\sigma_+^{A,B}\sigma_-^{A,B}, \tag{11}$$

and thus the dipole operators can be decomposed into Pauli matrices as $\mathbf{d}_S = \sigma_x^S\mathbf{d}_x^S + \sigma_z^S\mathbf{d}_z^S + \mathbf{1}\mathbf{d}_1^S$

$$H_I = -\sum_{S=A,B}(\sigma_x^S\mathbf{d}_x^S + \sigma_z^S\mathbf{d}_z^S + \mathbf{1}\mathbf{d}_1^S)\cdot\mathbf{E}. \tag{12}$$

This shows that the permanent dipoles interact identically with the electromagnetic field as the transition dipoles.

To calculate the dipole-dipole coupling terms, it is informative to utilise the Coulomb gauge.

A. Coulomb Gauge

The Hamiltonian now has two dipoles. We label the dipoles by $i \in \{1, 2\}$, and each dipole has an electron and hole at positions $\mathbf{R}_{e_i} = \mathbf{R}_i + \mathbf{r}_i/2$ and $\mathbf{R}_{h_i} = \mathbf{R}_i - \mathbf{r}_i/2$ respectively. The associated Hamiltonian is then of the form

$$H = \sum_{\mu\in\{e_i,h_i\}} \Big[\frac{1}{2m_\mu}(\mathbf{p}_\mu - q_\mu \mathbf{A}_\perp(\mathbf{R}_\mu))^2 + v_c(\mathbf{R}_\mu)\Big] + U_{\text{elec}} + \sum_{\mathbf{k},n} \omega_{\mathbf{k}} a^\dagger_{\mathbf{k},n} a_{\mathbf{k},n}. \tag{13}$$

The electrostatic interaction is

$$U_{\text{elec}} = -\frac{1}{2}\int d^3x \mathbf{E}_L^2(x) = U_{11} + U_{22} + 2U_{12}, \tag{14}$$

where $\mathbf{E}_L(x) = \sum_i \mathbf{E}_{iL}(x)$ are the longitudinal electric fields sourced by the dipoles, and $\mathbf{E}_{iL}(x) = \sum_{\mu\in\{e_i,h_i\}} \mathbf{E}_{\mu L}(x)$ are the longitudinal fields sourced by the constituent charges. Again, we have defined the electrostatic self-interactions of the dipoles, $U_{ii} = U_{e_i-e_i} + U_{h_i-h_i} + 2U_{e_i-hi}$ and we will ignore the self-charge energies as is standard. We now have inter-dipole electrostatic interactions

$$U_{12} = -\frac{1}{2}\int d^3x \mathbf{E}_1^{||}(x) \cdot \mathbf{E}_2^{||}(x), \tag{15}$$

which yields under the electric dipole approximation

$$V \equiv 2U_{12} = \frac{\mathbf{d}_1 \cdot \mathbf{d}_2 - 3(\mathbf{d}_1 \cdot \hat{\mathbf{R}}_{12})(\mathbf{d}_2 \cdot \hat{\mathbf{R}}_{12})}{4\pi\epsilon_0 |\mathbf{R}_{12}|^2}. \tag{16}$$

Projecting onto the two-level Hilbert space for each subsystem amounts to replacing $\mathbf{d}_i$ with $\sigma_x^{(i)}\mathbf{d}_x^{(i)} + \sigma_z^{(i)}\mathbf{d}_z^{(i)} + \mathbf{1}\mathbf{d}_1^{(i)}$. For strongly coupled dipole systems it has been shown that one should take the dipole coupling directly into the system Hamiltonian [**?**] and as such we have derived the Hamiltonian used above.

II. Transition Rates

In the permanent dipole molecular chain Hamiltonian we have introduced several new interaction terms into our model, here we will explore the collective permanent dipole-electromagnetic field interaction. Due to the σ_z nature of the operator interaction, we anticipate that this interaction will lead to transitions in the single excitation manifold, much in the same way as phonon relaxation. However, unlike the phonon baths that are independent for each site in the chain, the electromagnetic environment is shared across all the sites. As such, we anticipate that this will lead to a N-dependent rate enhancement when compared to the phonon relaxation. To this end, we consider the transition from the optically bright symmetric state

$$|\Psi_B\rangle = \frac{1}{\sqrt{N}}\sum_{j=1}^{N} |j\rangle\,, \tag{17}$$

to an optically dark state

$$|\Psi_D\rangle = \frac{1}{\sqrt{N}}\sum_{j=1}^{N} (-1)^j |j\rangle\,. \tag{18}$$

To calculate the coupling strength between these states due to phonon interactions we first calculate the single-site coupling

$$\begin{aligned} B^n_{\text{vib}} &= |\langle\Psi_D| \sigma_z^{(n)} |\Psi_B\rangle|^2 \\ &= \left|\frac{1}{N} 2(-1)^n\right|^2 = \frac{4}{N^2}, \end{aligned} \tag{19}$$

where we have assumed an even number of sites in the chain. As each of the phonon baths are uncorrelated it suffices to simply sum the transition rates from each bath

$$B_{\text{vib}} = \sum_{n=1}^{N} B^n_{\text{vib}} = \frac{4}{N}. \tag{20}$$

From this, it is clear to see that the transition rate to any specific dark state is suppressed by the number of sites in the chain. However, as the number of dark states is $N-1$, the overall scaling of decay from the bright state to the dark manifold becomes independent of N. Now we shall consider the same transition due to the permanent dipole interaction with the electromagnetic field. Due to the collective field, the transition element takes the form

$$\begin{aligned} B_{\text{opt}} &= \left|\langle\Psi_D| \sum_{n=1}^{N} \sigma_z^{(n)} \mathbf{d}_z^{(n)} |\Psi_B\rangle\right|^2 \\ &= \frac{4}{N^2}\left|\sum_{k=1}^{N} (-1)^k \mathbf{d}_z^{(k)}\right|^2. \end{aligned} \tag{21}$$

By considering alternating permanent dipoles $\mathbf{d}_z^{(n)} = \mathbf{d}_z(-1)^n$, such that

$$B_{\text{opt}} = \frac{4}{N^2}|N\mathbf{d}_z|^2 = 4|\mathbf{d}_z|^2\,. \tag{22}$$

This is an optimal configuration as it saturates the triangle inequality. This rate scales independent of N and we can note that the ratio between the vibrational transition

and the optical transition elements is linear in N

$$\frac{B_{\text{opt}}}{B_{\text{vib}}} \propto N. \tag{23}$$

This analysis shows that we anticipate that the effects of permanent dipole driving to dark states will play an important role as the number of sites increases. It will start to play a significant role when $N \approx \frac{\gamma_{\text{vib}}}{\gamma_{\text{opt}}}$, where $\gamma_{\text{opt,vib}}$ are the decay rates associated with the optical and vibrational environments discussed further in the next section. Furthermore, the analysis undertaken here assumes that the dark and bright states of a chain with no dipole-dipole coupling are appropriate analogues for the eigenstates of the chain system considered. This is a reasonable assumption for weak dipole couplings as we assume that the effects of dipole-dipole interactions act as small perturbations and as such the general results still hold. One should note that whilst we have a N scaling of the transition rate associated with going from the bright state to the specific dark state we have chosen here, we should note that this is optimised for this specific dark state. In a similar way to how the bright states accumulate oscillator strengths from the dark states, we can understand this transition as accumulating transition strength from other dark states. Thus the overall decay into the dark manifold is conserved. This, however, is still an interesting result as one could anticipate extraction occurring from a specific dark state due to dipole geometries and optimising populating a single dark state could prove beneficial.

III. Zero temperature detuning effects

In order to validate that some dipole configurations utilise a central manifold hopping to reach the end sites we show the case in which such hopping is not possible by bringing both the phonon and photon baths to zero temperature, such that absorption (upwards) rates are 0. This is shown in Fig. 1, where compared with the room temperature configuration outlined in the main text, we clearly see suppression of the $\uparrow\rightarrow$ configuration, evidencing its transport through the raised central manifold.

IV. Dynamics for Non-Radiative Decay

In order to study the effects of how non-radiative decay impacts the steady-state current we consider the dynamics of the configurations outlined in the main paper. These are relevant as the dynamical timescale over which excitations are transferred through the network will determine whether or not certain degrees of non-radiative decay will inhibit energy transport. As if excitations reach the end-site after a time τ_f, then non-radiative decay rates of $\Gamma_{NR} \approx \tau_f^{-1}$ will greatly suppress transport. The results of these simulations are shown in Fig. 2,

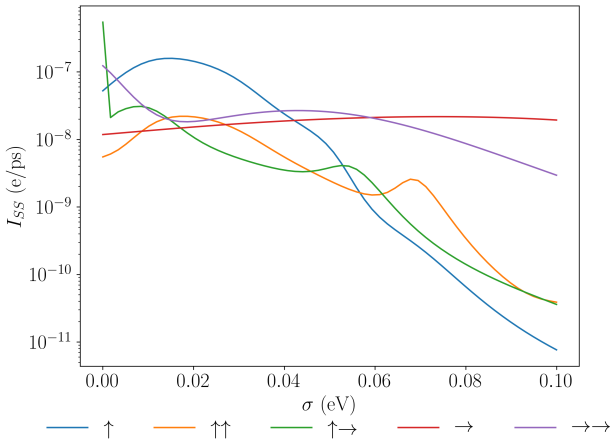

FIG. 1: Steady state current for different dipole configurations at zero temperature. Varying the static disorder within the system with site energies shifted by a value sampled from a normal distribution with standard deviation σ. Averages taken over 400 samples.

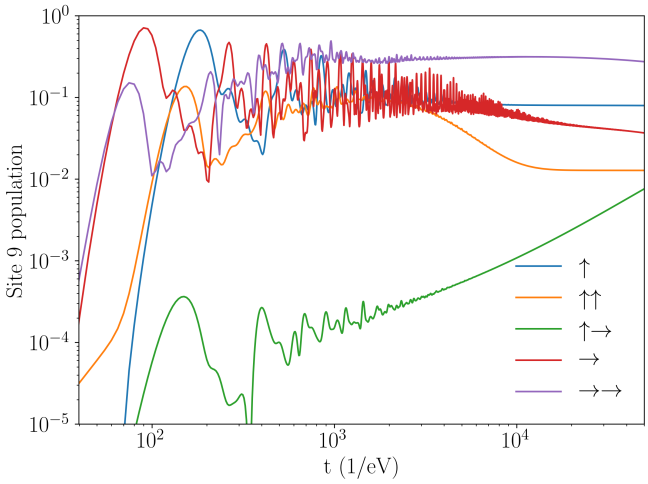

FIG. 2: Dynamics of population of the end site of a chain with an excitation initially in the first site, for varying dipole configuration.

where we have started with an excitation in the first site and removed non-radiative decay ($\Gamma_{NR} = 0$) to see these timescales. We note that the $\rightarrow\rightarrow$ configuration reaches a quasi-equilibration at a higher value more quickly and thus will be less sensitive to non-radiative decay.

V. ENAQT without radiative and non-radiative decay

Here we explore the ability for the dipole chain to utilise environmental noise assisted quantum transport (ENAQT) when we remove difference loss mechanisms

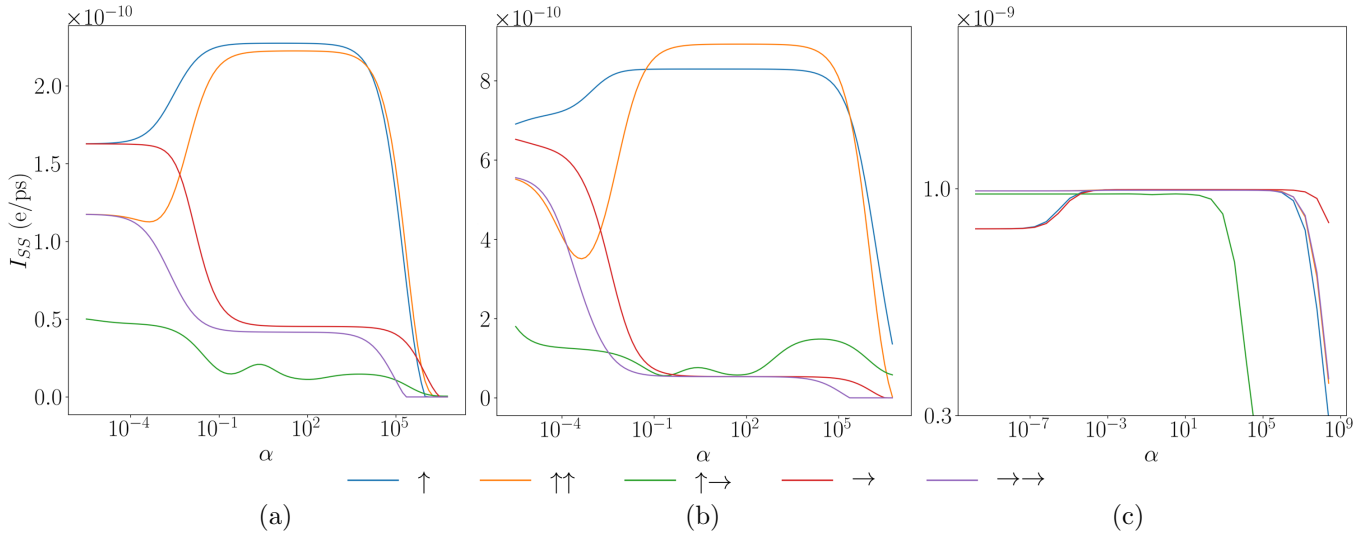

FIG. 3: Plots of the steady state current due to extraction of the end site of a molecular dipole chain for different dipolar configurations. Varying the relative strength of the vibrational coupling to the dipoles. (a) With non-radiative and radiative decay (b) With radiative decay and without non-radiative decay (c) Without non-radiative and radiative decay. The inset depicts a dipole chain with vibrational effects at each site along the chain.

from the network. This will enable the discussion of how explicit losses impact the generality of the scheme. In Fig. 3, we show the impact of removing non-radiative decay and photon losses from the network on the ability for the system to utilise the ENAQT scheme.